# Catalysts based on nickel salt heteropolytungstates for selective oxidation of diphenyl sulfide

M. Munoz, M. Greber, Karima Ben Tayeb Meziane, Carole Lamonier, C. I.
Cabello, G. P. Romanelli, M. Greber

Research Article

Mercedes Muñoz*, Matthieu Greber, Karima Ben Tayeb, Carole Lamonier, Carmen I. Cabello, and Gustavo P. Romanelli*

# Catalysts based on nickel salt heteropolytungstates for selective oxidation of diphenyl sulfide

**Abstract:** Nickel salts of Keggin heteropolytungstates with the general formula $Ni_xA_yW_{12-y}O_{39 or 40}$ (A = Si/P) were synthesized and studied as bulk catalytic materials or supported ones by deposition on modified and functionalized clay minerals (pillared layered clay and porous clay heterostructure). Characterizations by Raman, $^{31}P$ and $^{29}Si$-NMR, and ESEM-EDS techniques showed that pure and supported systems preserved the Ni/W ratio and the expected structural properties of heteropolyanions. These materials were evaluated as catalysts in the selective oxidation of sulfides to sulfoxides or sulfones, using aqueous hydrogen peroxide and mild reaction conditions. The bulk materials, with a higher content of Ni, displayed a remarkable catalytic behavior in the oxidation of diphenyl sulfide ($Ni_3PW_{11}NiO_{40}H$, 90% conversion in 15 min at 75°C, 100% sulfone selectivity in 3 h). Supported catalysts, particularly the non-functionalized PCH ($Ni_2SW_{12}O_{40}/PCH$), showed excellent activity, with also being selective in the oxidation of sulfide to sulfoxide (87% conversion, 88.9% sulfoxide selectivity). The reuse of these materials was studied in the optimum reaction conditions, resulting in similar activity and selectivity.

**Keywords:** phosphoro/silicoheteropolyanions, Ni(II) Keggin heteropolytungstates, modified clays, clean oxidation, diphenyl sulfide

## 1 Introduction

Particularly over the past few years, ongoing and strict amendments to environmental regulations have been directed for reducing the sulfide content in petroleum products [1–3]. The hydrodesulfurization (HDS) process generally used to remove sulfur is a high-cost process that involves high temperatures and pressures, larger volume reactors, and the use of very active catalysts [4–6]. Regarding the treatment of petroleum products, studies on oxidative desulfurization (ODS), a strategy proposed as an alternative or complementary to the HDS, have been reported. The oxidation of aromatic sulfides could be an interesting method to comply with the forthcoming regulations to obtain "0" sulfur fuels [7]. Moreover, another major problem facing the chemical industry is the enormous amount of waste that contains organic sulfur compounds, so the oxidation of sulfides has recently attracted enormous interest [8].

On the other hand, the selective oxidation of aromatic compounds is also important for the pharmaceutical industry to obtain commodity chemical products such as sulfone and/or sulfoxide substances, which are easily removable by conventional separation methods. Both sulfoxides and sulfones are important intermediate compounds in the pharmaceutical industry, food industry, etc. They are used as additives in crop protection, veterinary drug, and industrial lubricants [9–14]. For example, sulfone derivatives have been used as precursor in the synthesis of algaecide, bactericide, and fungicide; in the treatment of diabetes, leprosy, and malaria; and in dermatology or precursors of antibiotics [9–15].

* **Corresponding author: Mercedes Muñoz,** Centro de Investigación y Desarrollo en Ciencias Aplicadas, Dr. J.J. Ronco, CINDECA-CCT La Plata CONICET-CIC-UNLP, Calle 47 No 257, 1900, La Plata, Buenos Aires, Argentina, e-mail: mmercedes@quimica.unlp.edu.ar
* **Corresponding author: Gustavo P. Romanelli,** Centro de Investigación y Desarrollo en Ciencias Aplicadas, Dr. J.J. Ronco, CINDECA-CCT La Plata CONICET-CIC-UNLP, Calle 47 No 257, 1900, La Plata, Buenos Aires, Argentina, e-mail: gpr@quimica.unlp.edu.ar
**Matthieu Greber:** Unité de Catalyse et Chimie du Solide - UCCS UMR CNRS 8181, Université des Sciences et Technologies de Lille, Bât. C3, 59655 Villeneuve d'Ascq Cedex, France
**Karima Ben Tayeb, Carole Lamonier:** Laboratoire de Spectrochimie Infrarouge et Raman - LASIR UMR CNRS 8516, Université de Lille 1, Bât. C4, 59655 Villeneuve d'Ascq Cedex, France
**Carmen I. Cabello:** Centro de Investigación y Desarrollo en Ciencias Aplicadas, Dr. J.J. Ronco, CINDECA-CCT La Plata CONICET-CIC-UNLP, Calle 47 No 257, 1900, La Plata, Buenos Aires, Argentina; Facultad de Ingeniería, UNLP, Calle 1 y 47 s/n, 1900 La Plata, Buenos Aires, Argentina

Environmentally safe methods need to be developed for selective oxidation or sustainable oxidation of sulfides, especially with mild procedures [15].

Peroxides are oxidants where oxygen is easily accessible and produce nonpolluting residues, and they are easy to store and are inexpensive. Processes including oxygen donors such as $H_2O_2$, which allows the performance of reactions in aqueous solution (in batch) or *tert*-butyl hydroperoxide (*t*-BuOOH), have recently been reported to improve environmental efficiency [7,10,16–18]. However, hydrogen peroxide alone is a relatively weak electrophile, and catalytic activation is additionally required [9].

The reaction efficiency increases notably in the presence of a catalyst. Homogeneous catalysts were commonly used in the ODS process due to the high efficiency of the one-phase catalytic system. The main types of homogeneous catalysts reported in the literature are carboxylic acids (formic and acetic acids) as well as homogeneous metallic systems such as polyoxometallates (POMs). The POM catalysts used in ODS process are salts of transition metals (V, W, Mo) that form peroxo complexes, improving catalytic performances, but sometimes POMs have heavy metals, such as Cr and Mn salts, which are environmentally unfriendly and generate a massive amount of harmful waste products [19]. Oxo–peroxo complexes of tungsten(VI) ion with a closed-shell electronic structure and $d^0$ configuration are important for their utilization as catalysts in the oxidation of phenols, and sulfides, as well as in the epoxidation of olefins. Generally, the oxo–peroxo complexes of transition metals have attracted special attention due to their importance in different fields [7,8,14]. By comparing the efficiency of heteropolyanions in the catalytic system, it was found that tungsten-based heteropolyanions were more active than those based on molybdenum, and another advantage of tungsten compounds over other heavy metals is their low toxicity [8,9]. The main disadvantage of POMs as catalysts is their high solubility in polar solvents, so they are difficult to be recovered and reused. This problem was overcome by their immobilization in appropriate porous materials with mean pore diameter and specific surface area [13,14].

In recent years, for oxidation reactions, attention has turned to heterogeneous catalytic systems. One of the advantages of heterogeneous systems is related to the easy product and catalyst separation, high productivity, and eco-compatibility.

In heterogeneous catalysts, the use of transition metals (molybdenum, vanadium, and tungsten) as active phases dispersed on various supports having acid properties has been reported. Various supports have been considered, including alumina, silica, and zeolites. There is also growing interest in molecular sieves such as mesoporous silicates, as well as activated carbon [18,19].

It has recently been observed that the incorporation of vanadium in the structure of Keggin-type silicopolyoxotungsto compounds improves their catalytic activity in sulfide oxidation due to the redox and acid properties of vanadium [14].

In recent work about $WO_x/ZrO_2$ and W-bronze catalytic systems, high conversion of diphenyl sulfide (DPS) and selectivity to diphenyl sulfone ($DPSO_2$) were obtained. These studies suggested that the presence of sites with different acid and redox characteristics gives these species a bifunctional character that favor the formation of a peroxo tungstate intermediate and the subsequent nucleophilic attack of the sulfur atom in the sulfide by peroxo species. In the same way, the existence of W intermediate peroxo species and their efficiency in this type of reaction has been proven [7,10].

Previously, a series of NiW-based heteropolyanions supported on amorphous silica-alumina has been studied as sulfide precursors and has proven to be efficient in "Hydrocracking" reactions [20,21]. Several tungstic, silicotungstic, and phospho-tungstic heteropolyanions, substituted or not by Ni(II), such as $Ni_{3/2}PW_{12}O_{40}$, $Ni_2SiW_{12}O_{40}$, $Ni_3H_2W_{12}O_{40}$, $Ni_3PW_{11}NiO_{40}H$, $Ni_4SiW_{11}O_{39}$ ($Ni_xA_yW_{12-y}O_{39or40}$ (A = Si or P)), were selected to be used in ODS reactions.

Potassium salts of lacunar Keggin $P/Si[W_{11}O_{39}]$ heteropolyanions were also used for comparison purposes.

Moreover, research on the utilization of clay minerals has a long history. As reported by Mao et al., although clay minerals are natural catalyst materials, many disadvantages, such as poor thermal stability and wide pore-size distributions, limit their applications. To bridge the gap between the properties of clays and the need for catalysts in the industry, materials based on modified clay minerals are necessary. Clays and their derivatives have become indispensable materials in many fields, such as high-technology areas, and industrial and agricultural production [22–25].

The layered alumino-silicates with swelling ability, such as bentonite, always contain negative charges on their layers because of the isomorphous substitution of the central atoms in the octahedral/tetrahedral sheet by cations of lower valence. These negative charges must be compensated by inorganic cations (e.g., Na(I) and Ca(II)). These inorganic cations are exchangeable and can be replaced with polycations and organic cations, and the resulting materials are denoted as pillared layered clays (PILCs) and organoclays, respectively. To improve thermal stability, porous clay heterostructures (PCHs) were obtained by incorporation of organosilane cations to organoclays and thermal treatment. The PCHs obtained are microporous

materials of high specific area. The PILCs show affinity toward hydrophilic inorganic compounds, and the organoclays toward hydrophobic organic compounds [22,26,27]. Natural and modified clays find extensive applications in organic synthesis. These materials, unlike other conventional catalysts, enjoy considerable advantages such as ease of handling, recyclability, low cost, and easier modulation of acidity levels by suitable exchange of cations, thus contributing to the main subject of "green chemistry" [22,23,28–31]. The easy work-up procedure and the reproducibility of the PCH synthesis make this system attractive for its potential application to large-scale operations.

In the present work, natural alumino-silicate bentonite type clay, chemically modified to be functionalized, was selected as support for the heteropolytungstate. A series of bulk NiW-based and clay-supported catalysts was studied in the ODS of a diphenyl compound to compare the effect of the presence of P or Si heteroatom, nickel content, and the use of supported and unsupported systems.
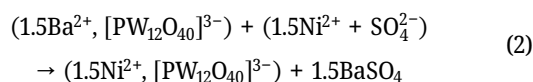
# 2 Materials and methods

## 2.1 Preparation of bulk catalysts

The preparation and characterization of Keggin-type phases substituted with Ni, $Ni_{3/2}PW_{12}O_{40}$, $Ni_2SiW_{12}O_{40}$, $Ni_3PW_{11}NiO_{40}H$, $Ni_4SiW_{11}O_{39}$, and $Ni_3H_2W_{12}O_{40}$ have recently been described [32]. Starting from the well-known heteropolyacid (HPAs) $H_3PW_{12}O_{40}$ and $H_4SiW_{12}O_{40}$, barium salts are synthesized according to Eq. 1 [33,34].

$$(3\,H^+, [PW_{12}O_{40}]^{3-}) + (1.5\,Ba^{2+}, 3OH^-)$$
$$\rightarrow (1.5Ba[PW_{12}O_{40}]^{3-}) + 3H_2O \tag{1}$$
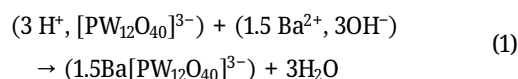
To obtain the nickel salts, the procedure consisted of successive incorporations of $NiSO_4$ solutions in stoichiometric amounts with respect to the corresponding solutions of the Keggin derivatives, under continuous stirring and at room temperature, according to Eq. 2 [32].

$$(1.5Ba^{2+}, [PW_{12}O_{40}]^{3-}) + (1.5Ni^{2+} + SO_4^{2-})$$
$$\rightarrow (1.5Ni^{2+}, [PW_{12}O_{40}]^{3-}) + 1.5BaSO_4 \tag{2}$$

The resulting solutions were then filtered to eliminate the $BaSO_4$ precipitate. Then, the solvent was evaporated at room temperature to obtain the Ni(II) salt.

The $[SiW_{12}O_{40}]^{4-}$ nickel salt was synthesized by the same procedure as that for $[PW_{12}O_{40}]^{3-}$ nickel salt. The formation of the lacunary species was due to the addition

of 3.5 equivalent of barium hydroxide (instead of 1.5). Indeed, the pH of the solution increased to 3, and the most stable species was $[PW_{11}O_{39}]^{7-}$ [32].

## 2.2 Synthesis of supports based on PCHs

The preparation was carried out according to conventional methods [27]. The starting material was bentonite-type natural clay, extracted from an Argentine deposit that was enriched in the montmorillonite fraction by the Stokes' method described previously [35,36]. This species is an aluminosilicate belonging to the group of smectites with a 2:1 laminar structure. Its structure is made up of two tetrahedral coordinated layers of $(Si,Al)O_4$ intercalated with an octahedral layer of $Al(O,OH)_6$ in which part of the Al is replaced by ions such as Mg or Fe. These 2:1 layers are negatively charged; in the clays, the neutrality is maintained by exchangeable cations such as Na(I) or Ca(II) [35].

The synthesis of the heterostructure material was conducted in several stages:

1. The natural material was first ion-exchanged to introduce sodium cations and then obtain sodium-based bentonite. For this, 2.00 g clay was suspended in 250 mL of NaCl solution (1 M) for 24 h, under stirring at room temperature. Then, the suspension was centrifuged, washed until a negative chloride reaction was obtained, and dried.

2. A treatment of the sodium-based bentonite with cetyltrimethylammonium bromide (Sigma-Aldrich; 95% HDTMA-Br) was applied to generate a cationic bentonite denoted as $B^+$. For this, 1.5 g Na-based bentonite was added to 150 mL of 0.5 mM solution of HDTMA-Br (NaB/HDTMA ratio = 1.5). The suspension was kept at 50°C under stirring for 24 h, then it was separated by centrifugation and washed until it reached pH = 7.

3. A reaction of the $B^+$ with Si precursor was performed. The $B^+$ obtained was suspended in a mixture of dodecylamine (DDA) and tetraethyl orthosilicate (TEOS; both from Aldrich) in $B^+$/DDA/TEOS (1.5 g $B^+$/7.56 g DDA/69.5 mL of TEOS). The suspension was stirred for 4 h at room temperature. The solid was separated by centrifugation and dried in air.

4. The material obtained in (3) was calcined at 550°C for 2 h to obtain the porous clay heterostructure material. The specific surface was determined using Micromeritics ASAP 2020 apparatus at the temperature of liquid nitrogen (−196°C) using a relative pressure range of 0.01–0.99. The specific surface area was estimated by the Brunauer–Emmett–Teller (BET) method. X-ray powder diffraction

(XRD) patterns were collected using Philips PW-1732 equipment (Cu Kα radiation, Ni filter).

## 2.3 Functionalization of the surface area of PCHs (PCH-F)

A functionalization process of the PCH systems [24] was conducted to increase their adsorption capacity to become an efficient support for HPA adsorption. The first step was a pretreatment of the materials to promote the availability of silanol groups; to this end, PCH was suspended in water/ethanol (50:50) for 24 h at room temperature and dried at 80°C. In the functionalization stage, the pretreated PCH (1.00 g) was mixed with the surfactant 3-aminopropyl-trimethoxysilane (F) in toluene as solvent at a rate according to the molecular weight of the surfactant and the $S_{BET}$ of the support ($S_{BET}$ PCH = 705 $m^2 \cdot g^{-1}$, PCH/F = 1 g/6.09 g·F).

The resulting suspension was stirred in a closed container at room temperature for 12 h and subsequently, the temperature was raised to 70°C for another 12 h. Finally, the suspension was filtered and washed with toluene and acetone. The solid was vacuum dried up to constant weight [24].

## 2.4 Preparation and characterization of catalysts supported on PCH and PCH-F

Supported catalysts were prepared by equilibrium impregnation in excess of pore volume, using 200 mg of PCH and PCH-F materials, and 2.4 mL of aqueous solutions of the phases containing W (100 $mg \cdot mL^{-1}$). To quantify the Ni on the PCH surface, the content of adsorbed Ni was calculated by mass balance from the initial and final content of Ni determined by atomic absorption spectroscopy (AAS) using Varian AA 240 equipment.

The solid (impregnated support) was dried in an oven at 70°C for 24 h and then it was used in an oxidation test. The catalyst Ni/W ratios were obtained by ESEM-EDS technique using a FEI Quanta 400 and EDAX Apollo 40 microscope, with ultra-thin energy dispersive window, which allows determination of light elements ($Z > 5$, from B). The analysis was conducted to corroborate textural properties and chemical composition.

## 2.5 Catalytic test

Catalytic tests were carried out using bulk and supported on PCH and PCH-F catalysts. The tests were based on the oxidation of DPS. The oxidation products potentially formed are diphenyl sulfoxide (DPSO) and $DPSO_2$. The reaction was carried out in batch at 75°C, using 0.01 mmol of catalyst, 1 mmol (0.186 g) of DPS, 5 mL of acetonitrile, and 1 mL of $H_2O_2$ 35% as oxidant. The catalytic assessment was followed by thin layer chromatography, analyzing samples at intervals of 15 min at the beginning of the analysis and 30 min in the final stage. Aliquots of 0.2 mL of the reaction mixture were also withdrawn at the same intervals. Each sample was extracted with dichloromethane/water (1 mL and 1 mL, respectively), and the organic phase was dried with anhydrous $Na_2SO_4$.

The organic phase was analyzed by gas chromatography (GC) on a Varian S*tart 3400cx* chromatograph equipped with a Chrompack column CP-sil 5 CB (30 m) and FID detector. The GC conditions were as follows: initial temperature was 50°C, ramped up to 210°C (at a rate of 20°C·$min^{-1}$ and temperature was constant for 1 min), and finally again ramped to 240°C (at a rate of 10°C·$min^{-1}$ and temperature was constant for 5 min). With this method, the corresponding retention times were: 11.1, 13.9, and 14.5 min for DPS, DPSO, and $DPSO_2$, respectively.

The reaction sample compositions were determined by area normalization method. From these values, the DPS conversion and selectivity values were obtained as a function of time.

# 3 Results and discussion

## 3.1 Catalyst characterization

The experimental Ni/W ratios determined by EDS in unsupported systems are reported in Table 1 and agree with the theoretical values based on the heteropolycompound stoichiometry.

**Table 1:** Data of theoretical and experimental Ni/W ratio for $Ni_xA_yW_{12-y}O_{40}$ (A = Si or P) HPA

| HPA | Ni/W (wt%/wt) | |
|---|---|---|
| | **Theoretical** | **EDS** |
| $Ni_4SiW_{11}O_{40}$ | 11.6 | 10.7 |
| $Ni_3H_2W_{12}O_{40}$ | 8.0 | 7.6 |
| $Ni_3PW_{11}NiO_{40}H$ | 11.6 | 16.1 |
| $Ni_{3/2}PW_{12}O_{40}$ | 4.0 | 3.4 |
| $Ni_2SiW_{12}O_{40}$ | 5.3 | 5.1 |
| $H_2O_2/H_2WO_4/NiW_3$ | 8.0 | 7.5 |
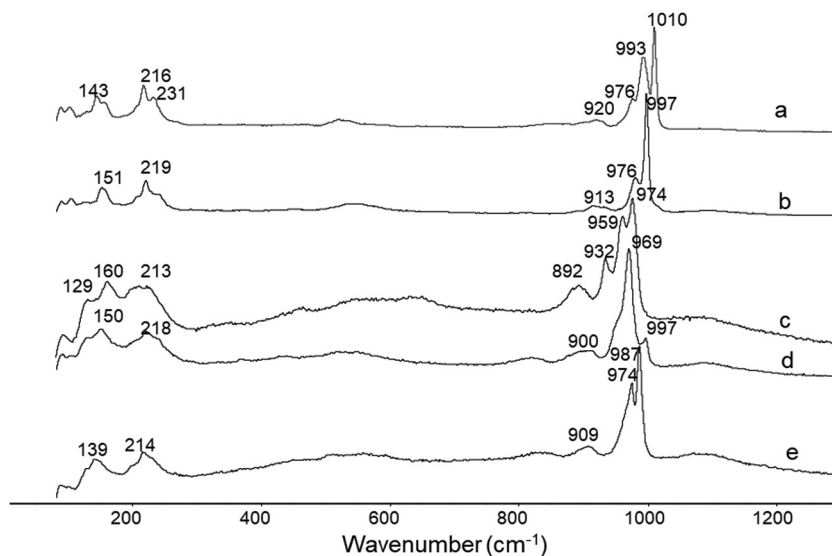
**Figure 1:** Raman spectra of: (a) $Ni_{3/2}PW_{12}O_{40}$, (b) $Ni_2SiW_{12}O_{40}$, (c) $Ni_3H_2W_{12}O_{40}$, (d) $Ni_4SiW_{11}O_{39}$, and (e) $Ni_3PW_{11}NiO_{40}H$ in aqueous solution.

Previous studies of Raman vibrational spectroscopy [32] in the systems $Ni_xA_yW_{12-y}O_{39 or 40}$ (A = Si or P) showed the preservation of the W–O terminal stretching modes at 1,011 and 998 cm$^{-1}$ that are characteristic of the $H_3PW_{12}O_{40}$ and $H_4SiW_{12}O_{40}$ phases used as starting material [37]. Thus, Raman spectra of Ni(II) salts (Figure 1) indicated that the Keggin structures $[PW_{12}O_{40}]^{3-}$ and $[SiW_{12}O_{40}]^{4-}$ were preserved after ionic exchange [32]. In Figure 1, $Ni_xA_yW_{12-y}O_{40}$ (A = Si or P) Raman spectra shows typical lines corresponding to W–$O_d$ stretching (terminal bond) at 1,010 cm$^{-1}$, W–$O_b$ ($\nu_{sym}$ and $\nu_{asym}$) stretching between 1,000 and 960 cm$^{-1}$, W–$O_b$–W bridges (890–850 cm$^{-1}$), W–$O_c$–W bridges (800–760 cm$^{-1}$), and lattice modes below 400 cm$^{-1}$, as reported by Ben Tayeb et al. [32]. The Ni(II) salt of $[PW_{11}NiO_{40}H]^{6-}$ did not exhibit the same line as that observed for $Ni_{3/2}PW_{12}O_{40}$, Figure 1a and b (respectively), but both presented a characteristic line at 989 cm$^{-1}$ corresponding to the W–$O_t$ stretching mode of the HPA. In the preparation procedure of this system, Ba(OH)$_2$ is added to raise the pH to pH < 3 where the Keggin anion is kinetically stable, and then a lacunary species is formed. The FT-IR spectroscopy (not presented in this work, see ref. [32]) confirmed the incorporation of Ni(II) to the structure of the $[PW_{11}NiO_{40}H]^{6-}$ anion. This fact indicated that the HPA structure did not change during the ion exchange to form the Ni(II) salt. A slight shift to lower frequencies can be observed when the H$^+$ is substituted by Ni(II). In the $Ni_4SiW_{11}O_{39}$ and $Ni_3PW_{11}NiO_{40}H$ systems (Figure 1d and e), the most intense Raman line shows that the W–O stretching is affected by the Si/P substitution (lacunar system). The general trend is a broadening and a shift to lower frequencies of the W–O point lines due to a decrease in symmetry. This can be attributed to the P or Si polarizing power that produces an

inductive effect, affecting the aforementioned type of W–O bonds [32].

^{31}P-NMR (Figure 2a) spectra showed the signal with chemical shift at −15.4 ppm, in agreement with values already reported for the $[PW_{12}O_{40}]^{3-}$ Keggin entities [38]. ^{31}P-NMR spectra (Figure 2b) for $Ni_{3/2}PW_{12}O_{40}$ species showed two signals at −15.4 and −13.1 ppm corresponding to phosphorus in $[PW_{12}O_{40}]^{3-}$ and $P_2W_{18}O_{62}^{6-}$ species, respectively [38]. A low decomposition (5%) seems to occur during the ionic exchange to form nickel salts. However, the Keggin structure is mainly preserved in the nickel salt $Ni_{3/2}PW_{12}O_{40}$. The [29]Si signal for $[SiW_{12}O_{40}]^{4-}$ was observed at −85.05 ppm (Figure 3b). The broad peak at −110 ppm presents the glass signal of the NMR probe. ^{29}Si-NMR analysis of the nickel salt of $[SiW_{11}O_{39}]^{8-}$ (Figure 3a) showed only one line at −85 ppm, clearly indicating



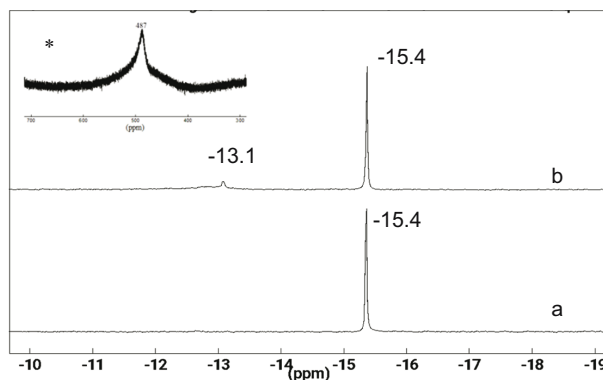**Figure 2:** ^{31}P-NMR spectra of (a) $H_3PW_{12}O_{40}$ and (b) $Ni_{3/2}PW_{12}O_{40}$ in aqueous solution at 5 × 10$^{-2}$ mol·L$^{-1}$. * $NiPW_{11}Ni$ for comparative purposes.
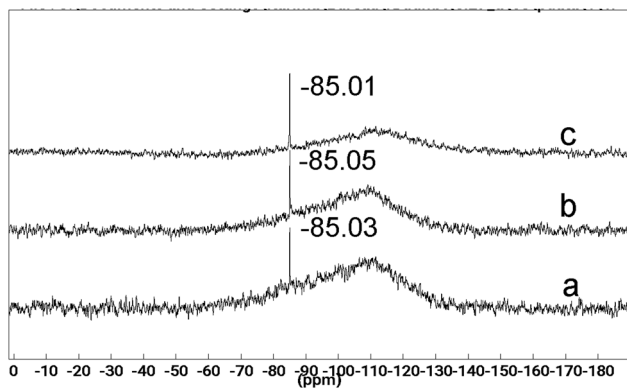
**Figure 3:** $^{29}$Si-NMR spectra of $Ni_4SiW_{11}O_{39}$ (a), $H_4SiW_{12}O_{40}$ (b), and $Ni_2SiW_{12}O_{40}$ (c) in aqueous solution at $5 \times 10^{-2}$ mol·L$^{-1}$.

that in the case of the Si based Keggin heteropolyanion, the paramagnetic nickel atom was not inserted in the HPA [39]. This chemical shift corresponds to $Ni_2SiW_{12}O_{40}$ species (Figure 3c). In fact, a low decomposition of $[SiW_{11}O_{39}]^{8-}$ on $[SiW_{12}O_{40}]^{4-}$ in aqueous solution occurred, whereas the absence of signal for $Ni_4SiW_{11}O_{39}$ lacunar species is due to the paramagnetic effect of Ni [21].

## 3.2 Support characterization

The XRD pattern of the selected bentonite corresponds mostly to sodium montmorillonite with the approximate formula: $(Na,Ca)_x(Al,Mg)_2Si_4O_{10}(OH)_2$ 4H$_2$O (PDF 291498) [35]. The XRD patterns are shown in Figure 4a. For the raw clay, the d001 diffraction peak can be observed at $2\theta = 6.7°$, which indicates that the cations located in the interlayer spacing are partially solvated [22]. In addition, the presence of narrower peaks also suggests the existence of impurities in the original bentonite. Thus, the presence of a peak
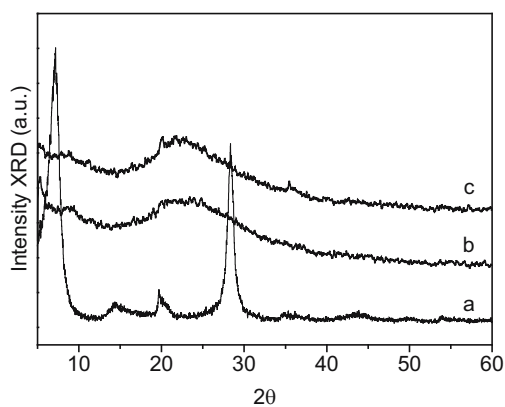


**Figure 4:** XRD patterns for (a) bentonite, (b) PCH, and (c) PCH-F materials.

located at around $2\theta = 7°$ is noteworthy, which is assigned for the existence of quartz, a phase that was eliminated during the Stokes purification process. In the PCH formation, the surfactant and TEOS treatments affect the total surface, leading to an increase in BET surface area and a decrease in crystallinity.

During the formation of PCH systems, the TEOS precursor is located between the clay basal planes due to an exchange reaction with the interlaminar cations Ca(II) and/or Na(I). After thermal treatment, precursor species were converted into "nanoscopic" oxide species that expand the distance between the alumina–silicate planes [35]. The diffraction peaks are less intense after the insertion of the pillars (Figure 4b), probably due to a partial delamination of the smectite, which causes a random displacement along the *a* and *b* axes leading to a house of cards structure [22].

In the process of PCH formation, the silica precursor (TEOS) generates an "*in situ*" polymerization with the surfactants intercalated between the clay films, and further treatment at 550°C removes the organic "templates" and high-surface area materials are generated, which are mainly microporous [35]. Thus, PCH materials of high surface area are obtained (Table 2), a noticeable increase in surface area occurred by organosilane incorporation. In previous studies of textural parameters, PCH porosity had an intermediate behavior between microporous materials, such as zeolites and pillared clays (pores <10 Å), and mesoporous materials (MCM-41, pores >20 Å). The IUPAC convention assigned a limit of 20 Å to micropore dimension [35].

The surface analysis of modified systems was carried out by ESEM-EDS microscopy (Table 2); the chemical treatment showed a Si/Al ratio variation. This ratio increased more than 2 times with the surfactant and TEOS treatment.

With the purpose of using PCH as support, the functionalization of these materials was conducted to achieve the surface adsorption of the heteropolyanions $Ni_xA_yW_{12-y}O_{40}$ (A = Si or P).

The surface Si–OH unities of the PCH materials was modified by functionalizing with 3-aminopropyltrimethoxysilane (F). The process follows the reaction of Scheme 1 [24].

**Table 2:** Textural parameters and EDS chemical data* of modified and functionalized clays

| Type of clay | $S_{BET}$ (m$^2$·g$^{-1}$) | Pore volume (cm$^3$·g$^{-1}$) | Si% | Al% | Si/Al |
|---|---|---|---|---|---|
| Bentonite | 22.5 | 0.02 | 80.11 | 19.89 | 4.00 |
| PCH | 705 | 0.56 | 89.46 | 10.54 | 8.50 |
| PCH-F | 18 | 0.20 | 94.75 | 5.25 | 18.00 |

*Data calculated from a content of Si + Al = 100%.
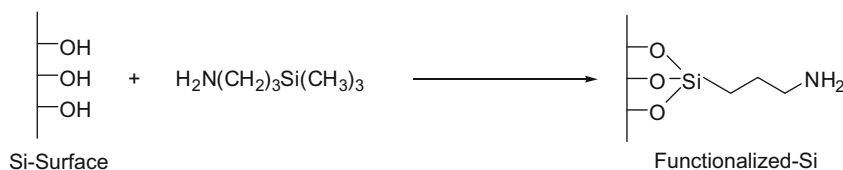
**Scheme 1:** Representation of the silica-surface functionalization process.

The XRD analysis (Figure 4) revealed that the functionalization process did not generate visible structural modifications in the clay matrix [24]. However, the functionalized systems showed a reduction in the surface area compared with the starting material (from $S_{BET}$ = 705–18 $m^2 \cdot g^{-1}$), probably because the process did not eliminate the surface Si–OH groups completely. This provides a certain degree of hydro-affinity to the surface by steric effect of the functionalizing agent, which could act as an umbrella protecting the surface silanol groups and reducing the surface area [24].

## 3.3 Supported catalysts

Regarding the preparation of the PCH and PCH-F based catalysts, the study of the Ni adsorption of these systems was conducted through mass balance by quantification of Ni by AAS in the $Ni_xA_yW_{12-y}O_{39or40}$ (A = Si or P) solutions before and after the impregnation process in equilibrium.

Table 3 shows experimental Ni/W ratios for the studied supported phases. A good agreement is observed between the Ni/W ratio determined from the pure phases and that of the supported systems obtained from EDS analysis. In the $Ni_2SiW_{12}O_{40}$ supported system, the Ni/W ratio is less reproducible due to the detection method capabilities when the concentration of the metals adsorbed in the matrix decreases. The adsorbed Ni(II) content increased by 10% (Table 3) in the cases in which functionalized systems were used as support.

## 3.4 Evaluation of the catalytic activity

The catalytic activity was investigated in the selective oxidation reaction of DPS in the presence of hydrogen peroxide as oxidant (35%), in acetonitrile as solvent, and assisted by the different catalysts under study (Scheme 2).

The reaction conditions (temperature, time, amount of catalyst and oxidant) were made as per previous studies [24]. The oxidation reaction in the absence of the catalyst occurred with very low sulfide conversions (10% after 3 h of reaction), and the resulting product was the intermediate sulfoxide DPSO, which showed incomplete oxidation.

**Table 3:** Bulk, theoretical, and experimental ratio of pure phases and supported on modified clays

| Bulk catalyst | Ni/W (wt%/wt) EDS | Supported catalyst | Ni/W (wt%/wt) EDS | Cad* Ni (%) AAS |
|---|---|---|---|---|
| $Ni_4SiW_{11}O_{39}$ | 10.7 | $Ni_4SiW_{11}O_{39}$/PCH-F | 10.6 | 3.62 |
| $Ni_3H_2W_{12}O_{40}$ | 7.6 | $Ni_3H_2W_{12}O_{40}$/PCH-F | 7.1 | 4.48 |
| $Ni_3PW_{11}NiO_{40}H$ | 16.1 | $Ni_3PW_{11}NiO_{40}H$/PCH-F | 10.0 | 0.70 |
| $Ni_{3/2}PW_{12}O_{40}$ | 3.4 | $Ni_{3/2}PW_{12}O_{40}$/PCH-F | 3.2 | 0.66 |
| $Ni_2SiW_{12}O_{40}$ | 5.1 | $Ni_2SiW_{12}O_{40}$/PCH-F | 0.2 | 0.43 |
| | | $Ni_2SiW_{12}O_{40}$/PCH | 0.2 | 0.33 |

*Cad: concentration of adsorbed Ni = {[($C_i - C_f$) × V]/m} × 100.
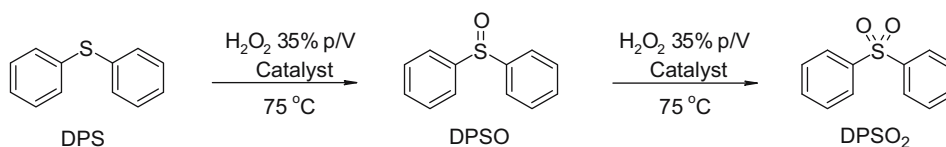


**Scheme 2:** Selective oxidation reaction of DPS to DPSO$_2$ in the presence of hydrogen peroxide as oxidant.

Figure 5 shows the catalytic results of pure and supported $Ni_xA_yW_{12-y}O_{39or40}$ (A = Si or P) catalysts in the oxidation of DPS at different reaction times.

All the $Ni_xA_yW_{12-y}O_{40or39}$ (A = Si or P) systems used as bulk catalysts show very good conversions (over 90%), except for the $Ni_4SiW_{11}O_{39}$ lacunar system, which showed lower conversion (70% in 3 h). In particular, the phase containing a higher Ni/W ratio showed the best performance. Likewise, all the systems were selective to $DPSO_2$ (over 75%) in 3 h of reaction, (Table 4, entries 1–5).

The evaluation of the conversion of DPS at short times (15 min), and under identical reaction conditions, shows that the $Ni_3PW_{11}NiO_{40}H$ catalyst was the most active (90% conversion, orange line in Figure 5), this effect being associated with Ni content determined by EDS (Table 3). This catalyst showed 100% selectivity towards sulfone after 3 h of reaction (Table 4, entry 5).

The $Ni_3H_2W_{12}O_{40}$ needed a longer reaction time to reach the maximum conversion, presenting the greatest induction period of all the systems. These results agree with the well-known effect of peroxide complex formation, such as $(PO_4[WO(O_2)_2]_4)$ type, which are intermediate species that catalyze the oxidation reactions studied [10]. The sulfides are oxidized to sulfoxides by electrophilic oxidants. The interaction of peroxide with W catalytic system generates an electrophilic intermediate (peroxo oxygen/metal), which attacks the sulfur atom generating the corresponding sulfoxide. Mechanistically, it is believed that the electrophilicity of the peroxide oxygen of $H_2O_2$ is increased by an oxometal group ($M=O_d$) in the $Ni_x(P/Si)_yW_{12-y}O_{40}$. And for the oxidation of sulfoxide to sulfone, the mechanism involves the nucleophilic attack of the oxygen in the sulfoxide to the tungsten atom in the $Ni_x(P/Si)_yW_{12-y}O_{40}$ with the formation of a Ni(P/Si)W-sulfoxide

**Table 4:** Selectivity (%) obtained at 3 h after DPS oxidation reaction in the presence of $H_2O_2$ using the bulk and supported $Ni_xA_yW_{12-y}O_{40}$ (A = Si or P) systems as catalysts

| | Catalyst | DPS conv. (%) | Selectivity, 3 h | |
| --- | --- | --- | --- | --- |
| | | | DPSO | DPSO$_2$ |
| 1 | $Ni_3H_2W_{12}O_{40}$ | 100 | 25.8 | 74.2 |
| 2 | $Ni_2SiW_{12}O_{40}$ | 98 | 0.8 | 99.2 |
| 3 | $Ni_4SiW_{11}O_{39}$ | 70 | 22.6 | 77.4 |
| 4 | $Ni_{3/2}PW_{12}O_{40}$ | 96 | 3.9 | 96.1 |
| 5 | $Ni_3PW_{11}NiO_{40}H$ | 100 | — | 100 |
| 6 | $Ni_2SiW_{12}O_{40}/PCH$ | 97 | 88.9 | 11.1 |
| 7 | $Ni_2SiW_{12}O_{40}/PCH-F$ | 100 | 36.5 | 63.6 |
| 8 | $Ni_3H_2W_{12}O_{40}/PCH-F$ | 100 | — | 100 |
| 9 | $Ni_4SiW_{11}O_{39}/PCH-F$ | 94 | 56.7 | 43.3 |
| 10 | $Ni_3PW_{11}NiO_{40}H/PCH-F$ | 99 | 4.8 | 95.2 |

intermediate and then, a nucleophilic attack of $H_2O_2$ on the sulfur atom in Ni(P/Si)W-sulfoxide via an $SN_2$ mechanism. The presence of Ni(II) metals in the structure introduces redox sites in the Keggin structure, giving a bifunctional character to these species, favoring the formation of peroxo tungstate intermediates [10,14,24].

Functionalized PCHs were also used as support to promote the adsorption of heteropolyanions. $Ni_2SiW_{12}O_{40}$ was also studied on non-functionalized PCH. Figure 5b shows the conversions for these supported systems, which are lower than those obtained for bulk catalysts after 1 h of reaction. After 2 h, better results are achieved for supported catalysts with conversion values above 80%. Moreover, the supported $Ni_4SiW_{11}O_{39}$ system presents a higher conversion than that of the corresponding bulk heteropolycompound, 94% and 70% of conversion in 3 h, respectively (Table 4, entries 3 and 9). The dispersion of the
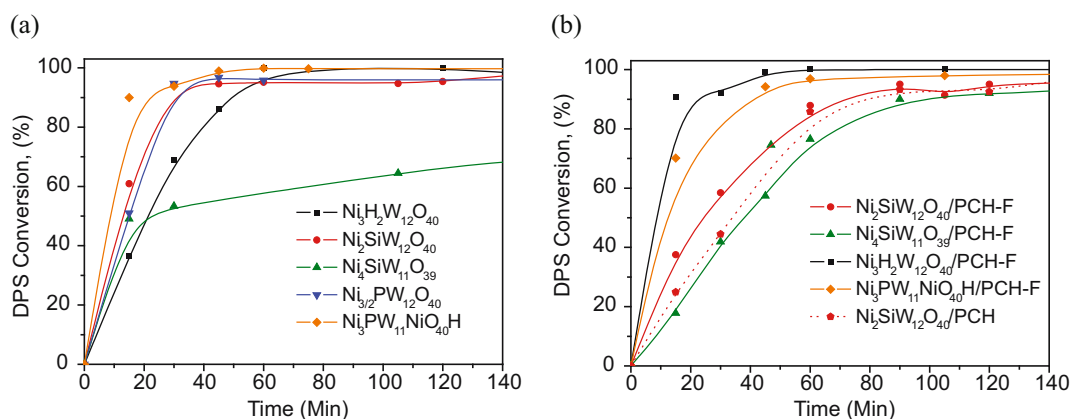


**Figure 5:** Dependence of conversion on the reaction time in the $Ni_xA_yW_{12-y}O_{40or39}$ (A = Si or P) bulk-catalyzed (a) and supported (b) selective oxidation of DPS.

bulk catalyst on the surface of the support generally leads to a decrease in activity; however, the $Ni_3H_2W_{12}O_{40}$/PCH-F catalyst also showed a significant increase in the conversion of the substrate (38% vs 92% in 15 min of reaction, black line in Figure 5). This again can be associated with the Ni content determined by AAS (the highest value found for all supported catalysts), as presented in Table 3. Another aspect of interest is related to the incorporation of the functionalizing agent. It was observed that the said treatment improves the nickel adsorption capacity and consequently, the activity of the catalyst and its selectivity towards the formation of sulfone. However, the non-functionalized PCH ($Ni_2W_{12}O_{40}$/PCH) showed excellent activity, being also selective in the oxidation of sulfide to sulfoxide (Table 4, entry 6).

Based on these results regarding the role of nickel in the catalytic system and knowing that the active species are the peroxo tungstate entities, we decided to conduct a comparative study of the Keggin lacunar phases with P or Si as heteroatom but containing K as countercation instead of Ni [10]. Finally, the evaluation of catalysts with a similar Keggin structure that do not contain Ni revealed that, although they are active (both bulk and supported catalysts), they are not selective for sulfoxide formation, the reaction product being sulfone. Table 5 and Figure 6 show the catalytic activity values under the same reaction conditions, applying potassium salts of lacunar Keggin structures.

The reusability of the catalysts was evaluated using the optimum reaction conditions. The catalyst was isolated from the reaction mixture, washed twice with the solvent (2 mL), dried under vacuum at 25°C until constant weight, characterized by Raman spectroscopy, and then reused in a new test. Raman spectra of the reused catalysts for the selected systems ($Ni_3PW_{11}NiO_{40}H$ and $Ni_2SiW_{12}O_{40}$) presented a good agreement in the position of the most intense lines (around 987, 974, and 909 $cm^{-1}$), without substantial changes in their structure, indicating the conservation of the heteropolyanion (Figure 7).



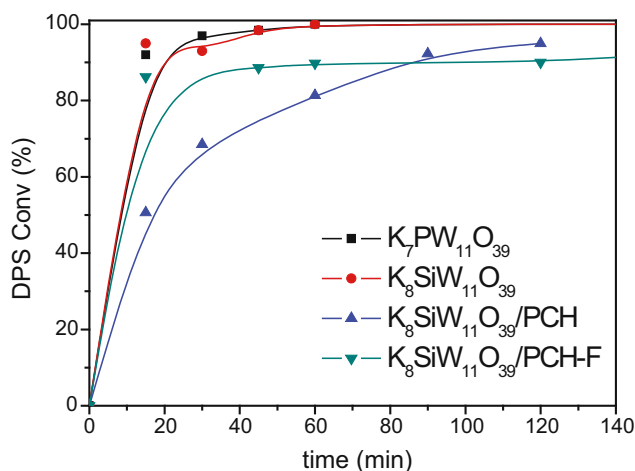**Figure 6:** Dependence of conversion on the reaction time in bulk and supported $K_xA_yW_{11}O_{39}$ (A = Si or P) in the selective oxidation of DPS.

No appreciable changes in conversion and selectivity values were detected when the treated catalyst was reused. The tests were performed with catalysts $Ni_3PW_{11}NiO_{40}H$, $Ni_2SiW_{12}O_{40}$, and $Ni_2SiW_{12}O_{40}$/PCH.

Finally, although slight differences are observed in the conversion rate between bulk and supported catalysts, it is expected that in the systems supported on PCH-F, the active phases will be more efficiently anchored, generating catalysts that are likely to be reused in several catalytic cycles.

As a general conclusion, it can be indicated that the incorporation of Ni in the Keggin-type structure generates bulk and supported materials that present very good

**Table 5:** Conversion and selectivity (%) at 3 h for the oxidation reaction of DPS in the presence of $H_2O_2$, using pure and supported $K_xA_yW_{12-y}O_{39}$ (A = Si or P) systems as catalysts

| Entry | Catalyst | DPS conv. (%) | Selec. (%) at 3 h | |
|---|---|---|---|---|
| | | | DPSO | DPSO$_2$ |
| 11 | $K_7PW_{11}O_{39}$ | 100 | 1.7 | 98.3 |
| 12 | $K_8SiW_{11}O_{39}$ | 100 | 0 | 100 |
| 13 | $K_8SiW_{11}O_{39}$/PCH | 93 | 3.0 | 97.0 |
| 14 | $K_8SiW_{11}O_{39}$/PCH-F | 95 | 2.1 | 98.0 |



**Figure 7:** Raman spectra after reaction for (a) $Ni_3PW_{11}NiO_{40}H$ and (b) $Ni_2SiW_{12}O_{40}$ selected systems.

activity and selectivity in the oxidation of DPS toward sulfone or alternatively towards the respective sulfoxide.

# 4 Conclusion

Supported catalysts, based on different Ni Keggin-type heteropolytungstates immobilized on chemically modified and functionalized Argentinean bentonite, were prepared. In the heterostructure systems, PCHs, a marked increase in the surface area and a decrease in the pore diameter were observed. The functionalization process allows the effective anchoring of the active phases. These were used as regenerable solid supports of different Ni Keggin-type heteropolytungstates.

The synthesized materials were evaluated as catalysts in the DPS oxidation to DPSO or sulfone, using aqueous $H_2O_2$ 35% w/v as green oxidant. They showed a great catalytic performance and selectivity under mild reaction conditions (75°C, using acetonitrile as reaction solvent). The evaluation of the conversion of DPS at short time of reaction revealed that the bulk $Ni_3PW_{11}NiO_{40}H$ catalyst was the most active (90% conversion, 100% sulfone selectivity), this result being associated with its Ni content. Dispersion of the catalyst on the surface of the support generally leads to a decrease in activity; however, in the case of the $Ni_3H_2W_{12}O_{40}$/PCH-F catalyst, a significant increase in the conversion of the substrate is observed when passing from bulk to supported catalysts (38–90%, 15 min). This can again be associated with the Ni content determined by AAS. The supported catalysts, particularly the non-functionalized PCHs, showed excellent activity and were also selective towards the formation of sulfone (97% conversion, 88.9% sulfoxide selectivity).

As a general conclusion, it can be indicated that the incorporation of Ni in the Keggin-type structure generates bulk and supported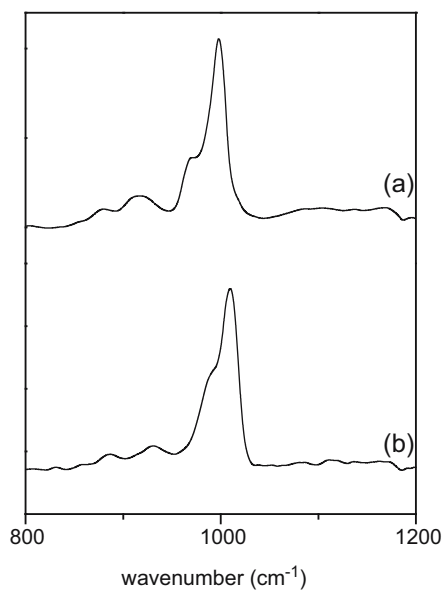 materials that present very good activity and selectivity in the oxidation of DPS towards sulfone or alternatively, towards the respective sulfoxide.

Advances in the activity of these Ni-based catalysts are beginning to be studied in our laboratory in relation to the recovery of building blocks present in biomass. Specifically, we have begun to study the selective oxidation reaction of furfural and 5-hydroxymethyl furfural, using eco-compatible oxidants such as hydrogen peroxide, and microwave radiation as an alternative source of energy.

**Author contributions:** Mercedes Muñoz: investigation, methodology, supervision, formal analysis, writing – original draft, and writing – review and editing. Matthieu Greber: investigation and methodology. Karima Ben Tayeb: investigation, methodology, supervision, formal analysis, and writing – original draft. Gustavo P. Romanelli: conceptualization, methodology, formal analysis, supervision, project administration, writing – original draft, and writing – review and editing. Carole Lamonier: conceptualization, methodology, project administration, supervision, formal analysis, writing – original draft, and writing – review and editing. Carmen I. Cabello: conceptualization, methodology, formal analysis, supervision, project administration, writing – original draft, and writing – review and editing.

# References

[1] Hossain MN, Park HC, Choi HS. A comprehensive review on catalytic oxidative desulfurization of liquid fuel oil. Catalysts. 2019;9:229. doi: 10.3390/catal9030229.

[2] Alvarez-Amparán MA, Cedeño-Caero L. $MoO_x$-$VO_x$ based catalysts for the oxidative desulfurization of refractory compounds: Influence of $MoO_x$-$VO_x$ interaction on the catalytic performance. Catal Today. 2017;282(2):133–9. doi: 10.1016/j.cattod.2016.07.002.

[3] Haghighi M, Gooneh-Farahani S. Insights to the oxidative desulfurization process of fossil fuels over organic and inorganic heterogeneous catalysts: Advantages and issues. Environ Sci Pollut R. 2020;27:39923–45. doi: 10.1007/s11356-020-10310-4.

[4] Campos-Martin JM, Capel-Sanchez MC. Catalytic oxidative desulfurization of liquid fuels. ACS Sym Ser. 2021;1379:3–174. doi: 10.1021/bk-2021-1379.ch006.

[5] Estephane G, Lancelot C, Blanchard P, Dufaud V, Chambrey S, Nuns N, et al. W-SBA based materials as efficient catalysts for the ODS of model and real feeds: Improvement of their lifetime through active phase encapsulation. Appl Catals A Gen. 2019;571:42–50. doi: 10.1016/j.apcata.2018.12.007.

[6] Bello SS, Wang C, Zhang M, Gao H, Han Z, Shi L, et al. A Review on the reaction mechanism of hydrodesulfurization and hydrodenitrogenation in heavy oil upgrading. Energ Fuel. 2021;35(14):10998–1016. doi: 10.1021/acs.energyfuels.1c01015.

[7] Muñoz M, Mendoza-Herrera LJ, Romanelli GP, Gazzoli D, Cabello CI. Catalytic behavior of the $WOx$-$ZrO_2$ system in the clean selective oxidation of diphenyl sulfide (DPS). Catal Today. 2021;372:146–53. doi: 10.1016/j.cattod.2020.10.011.

[8] Kargar H, Moghadam M, Shariati L, Bahadori M, Fallah-Mehrjardi M, Munawar KS. Green and efficient removal of sulfides using oxo-peroxo tungsten (VI)-MIL-101(Cr) nanoreactor as

heterogeneous recyclable catalyst. Inorg Chim Acta. 2023;545:121274. doi: 10.1016/j.ica.2022.121274.

[9] Brasil H, Gondim de Carvalho AL, Fernandes Costa F, Santos do Nascimento LA, Mhadmhan S, Pineda S, et al. Preparation of novel mesoporous Ca/P MCM-41-based materials for mechanochemical diphenyl sulfide oxidation. Microporous Mesoporous Mater. 2020;297:110017. doi: 10.1016/j.micromeso.2020.110017.

[10] Egusquiza MG, Soriano MD, Muñoz M, Romanelli G, Soriano J, Cabello CI, et al. Precursors of tetragonal tungsten bronzes as catalysts in selective reactions: Liquid phase oxidation of diphenyl sulfide and gas phase oxidation of hydrogen sulfide. Catal Today. 2021;372:70–81. doi: 10.1016/j.cattod.2021.05.001.

[11] Feng M, Tang B, Liang SH, Jiang X. Sulfur containing scaffolds in drugs: Synthesis and application in medicinal chemistry. Curr Top Med Chem. 2016;16(11):1200–16. doi: 10.2174/1568026615666150915111741.

[12] Bresciani G, Gemmiti M, Ciancaleoni G, Pampaloni G, Marchetti F, Crucianelli M. Niobium(V) oxido tris-carbamate as easily available and robust catalytic precursor for the selective sulfide to sulfone oxidation. Mol Cat. 2021;516:111972. doi: 10.1016/j.mcat.2021.111972.

[13] Sheng K, Huang XQ, Wang R, Wang WZ, Gao ZY, Tung CH, et al. Decagram-scale synthesis of heterometallic Ag/Ti cluster as sustainable catalyst for selective oxidation of sulfides. J Catal. 2023;417:185–93. doi: 10.1016/j.jcat.2022.12.007.

[14] Kargar H, Moghadam M, Shariati L, Feizi N, Fallah-Mehrjardi M, Behjatmanesh-Ardakani R, et al. Synthesis, crystal structure, spectral characterization, theoretical studies, and investigation of catalytic activity in selective oxidation of sulfides by oxo-peroxo tungsten(VI) Schiff base complex. J Mol Struc. 2022;1257:132608–26. doi: 10.1016/j.molstruc.2022.132608.

[15] Frenzel RA, Palermo V, Sathicq AG, Elsharif AM, Luque R, Pizzio LR, et al. A green and reusable catalytic system based on silicopolyoxotungstovanadates incorporated in a polymeric material for the selective oxidation of sulfides to sulfones. Microporous Mesoporous Mater. 2021;310:110584. doi: 10.1016/j.micromeso.2020.110584.

[16] Voutyritsa E, Triandafillidi I, Kokotos C. Green organocatalytic oxidation of sulfides to sulfoxides and sulfones. Synthesis. 2016;49(4):917–24. doi: 10.1055/s-0036-1588315.

[17] García-Gutiérrez JL, Laredo GC, García-Gutiérrez P, Jiménez-Cruz F. Oxidative desulfurization of diesel using promising heterogeneous tungsten catalysts and hydrogen peroxide. Fuel. 2014;138:118–25. doi: 10.1016/j.fuel.2014.07.049.

[18] Houda S, Lancelot C, Blanchard P, Poinel L, Lamonier C. Oxidative desulfurization of heavy oils with high sulfur content: A review. Catalysts. 2018;8:344. doi: 10.3390/catal8090344.

[19] Fang L, Xu Q, Qi Y, Wu X, Fu Y, Xiao Q, et al. Fe/Fe$_3$C@N-doped porous carbon microspindles templated from a metal–organic framework as highly selective and stable catalysts for the catalytic oxidation of sulfides to sulfoxides. Mol Cat. 2020;486:110863. doi: 10.1016/j.mcat.2020.110863.

[20] Saab R, Polychronopoulou K, Zheng L, Kumar S, Schiffer A. Synthesis and performance evaluation of hydrocracking catalysts: A review. J Ind Eng Chem. 2020;89:83–103. doi: 10.1016/j.jiec.2020.06.022.

[21] Ben Tayeb K, Lamonier C, Lancelot C, Fournier M, Payen E, Bonduelle A, et al. Study of the active phase of NiW hydrocracking sulfided catalysts obtained from an innovative heteropolyanion

based preparation. Catal Today. 2010;150(3–4):207–12. doi: 10.1016/j.cattod.2009.07.094.

[22] Cecilia JA, García-Sancho C, Vilarrasa-García E, Jiménez-Jiménez J, Rodriguez-Castellón E. Synthesis, characterization, uses and applications of porous clays heterostructures: A review. Chem Rec. 2018;18(7–8):1085–104. doi: 10.1002/tcr.201700107.

[23] Kooli F, Liu Y, Hbaieb K, Al-Faze R. Preparation and catalytic activities of porous clay heterostructures from aluminium-intercalated clays: Effect of Al content. Clay Miner. 2017;52(4):521–35. doi: 10.1180/claymin.2017.052.4.09.

[24] Muñoz M, Gallo MA, Gutiérrez-Alejandre A, Gazzoli D, Cabello CI. Molybdenum-containing systems based on natural kaolinite as catalysts for selective oxidation of aromatic sulfides. Appl Catal B Env. 2017;219:683–92. doi: 10.1016/j.apcatb.2017.08.007.

[25] Mao H, Li B, Li X, Yue L, Liu Z, Ma W, et al. Novel one-step synthesis route to ordered mesoporous silica-pillared clay using cationic-anionic mixed-gallery templates. Ind Eng Chem Res. 2010;49:583–91. doi: 10.1021/ie9011563.

[26] Zhu R, Wang T, Ge F, Chen W, You Z. Intercalation of both CTMAB and Al$_{13}$ into montmorillonite. J Colloid InterfaceSci. 2009;335:77–83. doi: 10.1016/j.jcis.2009.03.033.

[27] Cardona Y, Korili SA, Gil A. Understanding the formation of Al$_{13}$ and Al$_{30}$ polycations to the development of microporous materials based on Al$_{13}$- and Al$_{30}$-PILC montmorillonites: A review. Appl Clay Sci. 2021;203:105996. doi: 10.1016/j.clay.2021.105996.

[28] Chmielarz L, Kowalczyk AJ, Skoczek M, Rutkowska M, Gil B, Natkański P, et al. Porous clay heterostructures intercalated with multicomponent pillars as catalysts for dehydration of alcohols. Appl Clay Sci. 2018;160:116–25. doi: 10.1016/j.clay.2017.12.015.

[29] Nagendrappa G, Chowreddy RR. Organic reactions using clay and clay-supported catalysts: A survey of recent literature. Catal Surv Asia. 2021;25:231–78. doi: 10.1007/s10563-021-09333-9.

[30] Sathicq G, Musante L, Romanelli G, Pasquale G, Autino J, Thomas HJ, et al. Clean transesterification of β-ketoesters catalyzed by hybrid silica sol-gel. Stud Surf Sci Catal. 2006;162:227–34. doi: 10.1016/S0167-2991(06)80911-0.

[31] Sathicq G, Musante L, Romanelli G, Pasquale G, Autino J, Thomas HJ, et al. Transesterification of β-ketoesters catalyzed by hybrid materials based on silica sol–gel. Catal Today. 2008;455:133–5. doi: 10.1016/j.cattod.2007.11.016.

[32] Ben Tayeb K, Lamonier C, Lancelot C, Fournier M, Payen E, Bertoncini F, et al. Preparation of new oxidic precursors based on heteropolyanions for efficient hydrocracking catalysts. CR Chim. 2009;12:692–8. doi: 10.1016/j.crci.2008.10.020.

[33] Souchay P. Ions mineraux condenses. Paris: Masson et Cie, Ed.. 1969. p. 92.

[34] North EO. Inorganic syntheses. Vol. 1. New York: McGraw Hill Ed; 1939. p. 129–31. doi: 10.1002/9780470132326.

[35] Muñoz M, Sathicq AG, Romanelli GP, Hernández S, Cabello CI, Botto IL, et al. Porous modified bentonite as efficient and selective catalyst in the synthesis of 1,5-benzodiazepines. J Porous Mater. 2013;20(1):65–73. doi: 10.1007/s10934-012-9575-0.

[36] Gil A, Korili SA, Vicente MA. Recent advances in the control and characterization of the porous structure of pillared clay catalysts. Catal Rev-Sci Eng. 2008;50:153–221. doi: 10.1080/01614940802019383.

[37] Rocchiccioli-Deltcheff C, Fournier M, Franck R, Thouvenot R. Vibrational investigations of polyoxometalates. 2. Evidence for anion-anion interactions in molybdenum(VI) and tungsten(VI)

compounds related to the Keggin structure. Inorg Chem. 1983;22:207–16. doi: 10.1021/ic00144a006.

[38] Massart R, Contant R, Fruchart JM, Ciabrini JP, Fournier M. Phosphorus-31 NMR studies on molybdic and tungstic heteropolyanions. Correlation between structure and chemical shift. Inorg Chem. 1977;16(11):2916–21. doi: 10.1021/ic50177a049.

[39] Bonchio M, Bortolini O, Conte V, Sartorel A. Electrospray behavior of lacunary keggin-type polyoxotungstates $[XW_{11}O_{39}]^{p-}$ (X = Si, P): Mass spectrometric evidence for a concentration-dependent incorporation of an $MO^{n+}$ (M = $W^{VI}$, $Mo^{VI}$, $V^{V}$) unit into the polyoxometalate vacancy. Eur J Inorg Chem. 2003;2003:699–704. doi: 10.1002/ejic.200390096.